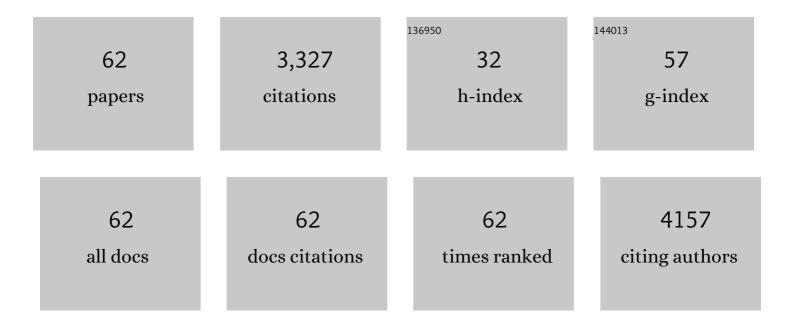
List of Publications by Year in descending order

Source: https://exaly.com/author-pdf/8274406/publications.pdf Version: 2024-02-01



YU MENC

#	Article	IF	CITATIONS
1	Modulating composite polymer electrolyte by lithium closo-borohydride achieves highly stable solid-state battery at 25°C. Science China Materials, 2022, 65, 95-104.	6.3	12
2	Selfâ€Adapting Electrochemical Grinding Strategy for Stable Silicon Anode. Advanced Functional Materials, 2022, 32, 2109887.	14.9	14
3	Sequential Phase Conversionâ€Induced Phosphides Heteronanorod Arrays for Superior Hydrogen Evolution Performance to Pt in Wide pH Media. Advanced Materials, 2022, 34, e2107548.	21.0	73
4	NiS1â^'xSex Nanoparticles Anchored on Nitrogen-Doped Reduced Graphene Oxide as Highly Stable Anode for Sodium-Ion Battery. Processes, 2022, 10, 566.	2.8	3
5	Alloying Co Species into Ordered and Interconnected Macroporous Carbon Polyhedra for Efficient Oxygen Reduction Reaction in Rechargeable Zinc–Air Batteries. Advanced Materials, 2022, 34, e2109605.	21.0	61
6	Respective Roles of Inner and Outer Carbon in Boosting the K ⁺ Storage Performance of Dual arbon onfined ZnSe. Advanced Science, 2022, 9, e2104822.	11.2	35
7	Interface Modification and Halide Substitution To Achieve High Ionic Conductivity in LiBH ₄ -Based Electrolytes for all-Solid-State Batteries. ACS Applied Materials & Interfaces, 2022, 14, 1260-1269.	8.0	9
8	Improved Lowâ€Temperature Performance of Rockingâ€Chair Sodiumâ€Ion Hybrid Capacitor by Mitigating the Deâ€Solvation Energy and Interphase Resistance. Advanced Functional Materials, 2022, 32, .	14.9	12
9	Less Is More: High-Performance All-Solid-State Electrode Enabled by Multifunctional MXene. ACS Applied Energy Materials, 2022, 5, 7210-7219.	5.1	4
10	In Situ Construction of Lithium Silicide Host with Unhindered Lithium Spread for Dendriteâ€Free Lithium Metal Anode. Advanced Functional Materials, 2021, 31, 2008786.	14.9	18
11	Ni, beyond thermodynamic tuning, maintains the catalytic activity of V species in Ni ₃ (VO ₄) ₂ doped MgH ₂ . Journal of Materials Chemistry A, 2021, 9, 8341-8349.	10.3	37
12	Two-Dimensional CuGaSe ₂ @ZnSe-NC Heterostructures for Enhanced Sodium Ion Storage. ACS Applied Energy Materials, 2021, 4, 2761-2768.	5.1	13
13	Stabilizing Transition Metal Vacancy Induced Oxygen Redox by Co 2+ /Co 3+ Redox and Sodiumâ€Site Doping for Layered Cathode Materials. Angewandte Chemie, 2021, 133, 22197-22205.	2.0	1
14	<i>P</i> â€Block Atomically Dispersed Antimony Catalyst for Highly Efficient Oxygen Reduction Reaction. Angewandte Chemie, 2021, 133, 21407-21411.	2.0	61
15	Stabilizing Transition Metal Vacancy Induced Oxygen Redox by Co ²⁺ /Co ³⁺ Redox and Sodium‧ite Doping for Layered Cathode Materials. Angewandte Chemie - International Edition, 2021, 60, 22026-22034.	13.8	39
16	<i>P</i> â€Block Atomically Dispersed Antimony Catalyst for Highly Efficient Oxygen Reduction Reaction. Angewandte Chemie - International Edition, 2021, 60, 21237-21241.	13.8	98
17	Co/CoP Heterojunction on Hierarchically Ordered Porous Carbon as a Highly Efficient Electrocatalyst for Hydrogen and Oxygen Evolution. Advanced Energy Materials, 2021, 11, 2102134.	19.5	138
18	A phosphorus and carbon composite containing nanocrystalline Sb as a stable and high-capacity anode for sodium ion batteries. Journal of Materials Chemistry A, 2020, 8, 443-452.	10.3	29

#	Article	IF	CITATIONS
19	Electrocatalytic Hydrogen Evolution of Ultrathin Coâ€Mo ₅ N ₆ Heterojunction with Interfacial Electron Redistribution. Advanced Energy Materials, 2020, 10, 2002176.	19.5	138
20	Revealing the Role of Liquid Metals at the Anode–Electrolyte Interface for All Solid-State Lithium-Ion Batteries. ACS Applied Materials & Interfaces, 2020, 12, 38232-38240.	8.0	13
21	Tailor-Made Gives the Best Fits: Superior Na/K-Ion Storage Performance in Exclusively Confined Red Phosphorus System. ACS Nano, 2020, 14, 12222-12233.	14.6	55
22	Conductive Boron Nitride as Promising Catalyst Support for the Oxygen Evolution Reaction. Advanced Energy Materials, 2020, 10, 1902521.	19.5	28
23	Li-triggered superior catalytic activity of V in Li ₃ VO ₄ : enabling fast and full hydrogenation of Mg at lower temperatures. Journal of Materials Chemistry A, 2020, 8, 14935-14943.	10.3	24
24	Rational Construction of Nitrogenâ€Doped Hierarchical Dual arbon for Advanced Potassiumâ€lon Hybrid Capacitors. Advanced Energy Materials, 2020, 10, 1904045.	19.5	197
25	Interfacial Charge Field in Hierarchical Yolk–Shell Nanocapsule Enables Efficient Immobilization and Catalysis of Polysulfides Conversion. Advanced Energy Materials, 2019, 9, 1901667.	19.5	59
26	Inside or Outside: Origin of Lithium Dendrite Formation of All Solid‧tate Electrolytes. Advanced Energy Materials, 2019, 9, 1902123.	19.5	76
27	Lithium Dendrites: Inside or Outside: Origin of Lithium Dendrite Formation of All Solid‣tate Electrolytes (Adv. Energy Mater. 40/2019). Advanced Energy Materials, 2019, 9, 1970155.	19.5	4
28	Embedding heterostructured MnS/Co _{1â^'x} S nanoparticles in porous carbon/graphene for superior lithium storage. Journal of Materials Chemistry A, 2019, 7, 1260-1266.	10.3	64
29	Exploring the sodium ion storage mechanism of gallium sulfide (Ga ₂ S ₃): a combined experimental and theoretical approach. Nanoscale, 2019, 11, 3208-3215.	5.6	24
30	Improving the Electrochemical Performance and Structural Stability of the LiNi _{0.8} Co _{0.15} Al _{0.05} O ₂ Cathode Material at High-Voltage Charging through Ti Substitution. ACS Applied Materials & Interfaces, 2019, 11, 23213-23221.	8.0	57
31	Fully reversible lithium storage of tin oxide enabled by self-doping and partial amorphization. Nanoscale, 2019, 11, 12915-12923.	5.6	12
32	Low-temperature electroless synthesis of mesoporous aluminum nanoparticles on graphene for high-performance lithium-ion batteries. Journal of Materials Chemistry A, 2019, 7, 13917-13921.	10.3	13
33	Unlocking the Lithium Storage Capacity of Aluminum by Molecular Immobilization and Purification. Advanced Materials, 2019, 31, e1901372.	21.0	23
34	A novel composite strategy to build a sub-zero temperature stable anode for sodium-ion batteries. Journal of Materials Chemistry A, 2019, 7, 9051-9058.	10.3	9
35	Controlled phase evolution from Cu _{0.33} Co _{0.67} S ₂ to Cu ₃ Co ₆ S ₈ hexagonal nanosheets as oxygen evolution reaction catalysts. RSC Advances, 2019, 9, 9729-9736.	3.6	11
36	A Highâ€Performance Li–B–H Electrolyte for Allâ€Solidâ€State Li Batteries. Advanced Functional Materials, 2019, 29, 1809219.	14.9	88

#	Article	IF	CITATIONS
37	Rooting bismuth oxide nanosheets into porous carbon nanoboxes as a sulfur immobilizer for lithium–sulfur batteries. Journal of Materials Chemistry A, 2019, 7, 7074-7081.	10.3	48
38	Cu 0.33 Co 0.67 S 2 Hexagonal Sheets with 2D Hierarchical Structures for Highâ€Rate and Longâ€Term Lithium Storage. ChemNanoMat, 2019, 5, 531-538.	2.8	3
39	Recent progress on printable power supply devices and systems with nanomaterials. Nano Research, 2018, 11, 3065-3087.	10.4	60
40	Rapid Amorphization in Metastable CoSeO ₃ ·H ₂ O Nanosheets for Ultrafast Lithiation Kinetics. ACS Nano, 2018, 12, 5011-5020.	14.6	53
41	Hierarchical Fe ₂ O ₃ @C@MnO ₂ @C Multishell Nanocomposites for High Performance Lithium Ion Batteries and Catalysts. Langmuir, 2018, 34, 5225-5233.	3.5	28
42	Tunable electronic coupling of cobalt sulfide/carbon composites for optimizing oxygen evolution reaction activity. Journal of Materials Chemistry A, 2018, 6, 10304-10312.	10.3	86
43	Magnesium Hydride Nanoparticles Self-Assembled on Graphene as Anode Material for High-Performance Lithium-Ion Batteries. ACS Nano, 2018, 12, 3816-3824.	14.6	41
44	CuGaS ₂ nanoplates: a robust and self-healing anode for Li/Na ion batteries in a wide temperature range of 268–318 K. Journal of Materials Chemistry A, 2018, 6, 1086-1093.	10.3	44
45	Embedding ZnSe nanodots in nitrogen-doped hollow carbon architectures for superior lithium storage. Nano Research, 2018, 11, 966-978.	10.4	114
46	Ultrafine Co Nanoparticles Encapsulated in Carbonâ€Nanotubesâ€Grafted Graphene Sheets as Advanced Electrocatalysts for the Hydrogen Evolution Reaction. Advanced Materials, 2018, 30, e1802011.	21.0	453
47	Hydrogen-induced magnesium–zirconium interfacial coupling: enabling fast hydrogen sorption at lower temperatures. Journal of Materials Chemistry A, 2017, 5, 5067-5076.	10.3	94
48	Pseudocapacitance-tuned high-rate and long-term cyclability of NiCo ₂ S ₄ hexagonal nanosheets prepared by vapor transformation for lithium storage. Journal of Materials Chemistry A, 2017, 5, 9022-9031.	10.3	87
49	General Synthesis of Dual Carbonâ€Confined Metal Sulfides Quantum Dots Toward Highâ€Performance Anodes for Sodium″on Batteries. Advanced Functional Materials, 2017, 27, 1702046.	14.9	259
50	CuO/ZnO/Al ₂ O ₃ Catalyst Prepared by Mechanical-Force-Driven Solid-State Ion Exchange and Its Excellent Catalytic Activity under Internal Cooling Condition. Industrial & Engineering Chemistry Research, 2017, 56, 8216-8223.	3.7	18
51	Bottom-up Approach Design, Band Structure, and Lithium Storage Properties of Atomically Thin \hat{I}^3 -FeOOH Nanosheets. ACS Applied Materials & Interfaces, 2016, 8, 21334-21342.	8.0	49
52	General Synthesis of Transition Metal Oxide Ultrafine Nanoparticles Embedded in Hierarchically Porous Carbon Nanofibers as Advanced Electrodes for Lithium Storage. Advanced Functional Materials, 2016, 26, 6188-6196.	14.9	61
53	Synthesis of Ammonia Borane Nanoparticles and the Diammoniate of Diborane by Direct Combination of Diborane and Ammonia. Chemistry - A European Journal, 2016, 22, 6228-6233.	3.3	14
54	Enhancement of Hydrogen Storage in Destabilized LiNH ₂ with KMgH ₃ by Quick Conveyance of N-Containing Species. Journal of Physical Chemistry C, 2016, 120, 1415-1420.	3.1	28

#	Article	IF	CITATIONS
55	Comparative Investigations on Hydrogen Absorption–Desorption Properties of Sm–Mg–Ni Compounds: The Effect of [SmNi5]/[SmMgNi4] Unit Ratio. Journal of Physical Chemistry C, 2015, 119, 4719-4727.	3.1	33
56	Advanced H ₂ -storage system fabricated through chemical layer deposition in a well-designed porous carbon scaffold. Journal of Materials Chemistry A, 2014, 2, 15168-15174.	10.3	6
57	Facile self-assembly of light metal borohydrides with controllable nanostructures. RSC Advances, 2014, 4, 983-986.	3.6	19
58	Carbon nanomaterial-assisted morphological tuning for thermodynamic and kinetic destabilization in sodium alanates. Journal of Materials Chemistry A, 2013, 1, 5238.	10.3	30
59	Superior Destabilization Effects of MnF ₂ over MnCl ₂ in the Decomposition of LiBH ₄ . Journal of Physical Chemistry C, 2011, 115, 13528-13533.	3.1	40
60	Improved dehydrogenation of TiF ₃ -doped NaAlH ₄ using ordered mesoporous SiO ₂ as a codopant. Journal of Materials Research, 2010, 25, 2047-2053.	2.6	19
61	Phase Stability, Structural Transition, and Hydrogen Absorptionâ^'Desorption Features of the Polymorphic La ₄ MgNi ₁₉ Compound. Journal of Physical Chemistry C, 2010, 114, 11686-11692.	3.1	83
62	Pressure hysteresis in the TiMn _{1.5} V <i>_x</i> -H ₂ (<i>x</i> = 0.1–0.5) system. Journal of Materials Research, 2009, 24, 2886-2891.	2.6	5